Metallography, Microstructure, and Analysis (2024) 13:1119–1130
https://doi.org/10.1007/s13632-024-01131-9

ORIGINAL RESEARCH ARTICLE

Material Studies on Decorative Buttons from the Hallstatt Period Tumuli in Mitterkirchen, Marchland, Upper Austria

Roland Haubner[1] · Susanne Strobl[1] · Jutta Leskovar[2]

Received: 21 April 2024 / Revised: 9 August 2024 / Accepted: 12 August 2024 / Published online: 11 September 2024

Abstract

The burial ground at Mitterkirchen belongs to the Early Iron Age, respectively, to the Hallstatt culture. A remarkable find from Mitterkirchen is approximately 3,000 buttons that were attached to a magnificent coat. Five of these buttons were provided for nondestructive material examinations using computed tomography (CT). Two of these buttons could be examined by metallography, light optical microscope (LOM), scanning electron microscope (SEM) with energy-dispersive X-ray analysis (EDX) and X-ray fluorescence examination (XRF). Based on the results of the investigation, it can be assumed that the bronze buttons were manufactured by a casting process. The bronze alloys are very different, which suggests the use of various starting materials including recycled copper alloys. The microstructure of the bronzes is uniform and, depending on their compositions, contains precipitates like Pb and the intermetallic phase $Cu_{41}Sn_{11}$. The corrosion layers exhibit a pronounced Sn enrichment and contain malachite.

Keywords Bronze · Buttons · Hallstatt period · Metallography

Introduction

The Iron Age is divided into the Early Iron Age (Hallstatt culture) and the Late Iron Age (Latène period). The site that gave the Hallstatt period its name is located in Upper Austria and is known for the oldest salt mine in the world [1]. In Upper Austria, numerous other important archeological sites from this period were found. These include, among others, the burial mounds of Helpfau-Uttendorf [2] and Gilgenberg-Gansfuß [3]. However, the best-known site from this period is the burial ground at Mitterkirchen [4, 5] (Fig. 1a).

The archaeological site near Mitterkirchen in Upper Austria is a large Hallstatt period burial ground, dated to the 8th century BC. In this period (Ha C), inhumation was predominant [6, 7]. The site was discovered because archaeological objects were repeatedly found as a result of intensive farming. However, before the unearthing started, some areas of the burial ground had already been destroyed. Nevertheless, during the archaeological excavations between 1980 and 1990 numerous sensational finds were discovered. Fifty tumuli and eighty burials were unearthed containing many burial objects [8, 9]. Noticeable was the find of approximately 3000 robe buttons that belonged to a ceremonial coat. It is assumed that the coat was made of leather, which naturally did not endure. The coat was reconstructed (Fig. 1b) [4]. Additionally two impressive chariots were found [4].

The metallurgy of copper extraction and bronze production have already been described in detail [10, 11]. The aim of material science studies on metallic artifacts is to find out details about the manufacturing process as well as the alloy composition [12]. In the present investigations, the question would be whether the buttons were produced directly by casting or by soldering or riveting individual parts. The very popular lead isotope analyses to determine the origin of the copper were not carried out, because such statements are impossible [13, 14].

The approximately 3,000 buttons from Mitterkirchen are undoubtedly special, but buttons were also found in other graves from this area [15, 16]. So far, buttons from a burial

✉ Roland Haubner
roland.haubner@tuwien.ac.at

Susanne Strobl
susanne.strobl@tuwien.ac.at

1 Institut für Chemische Technologien und Analytik, Technische Universität Wien, Getreidemarkt 9/164-03, 1060 Vienna, Austria

2 Oberösterreichisches Landesmuseum (OÖLKG), Leonding, Austria

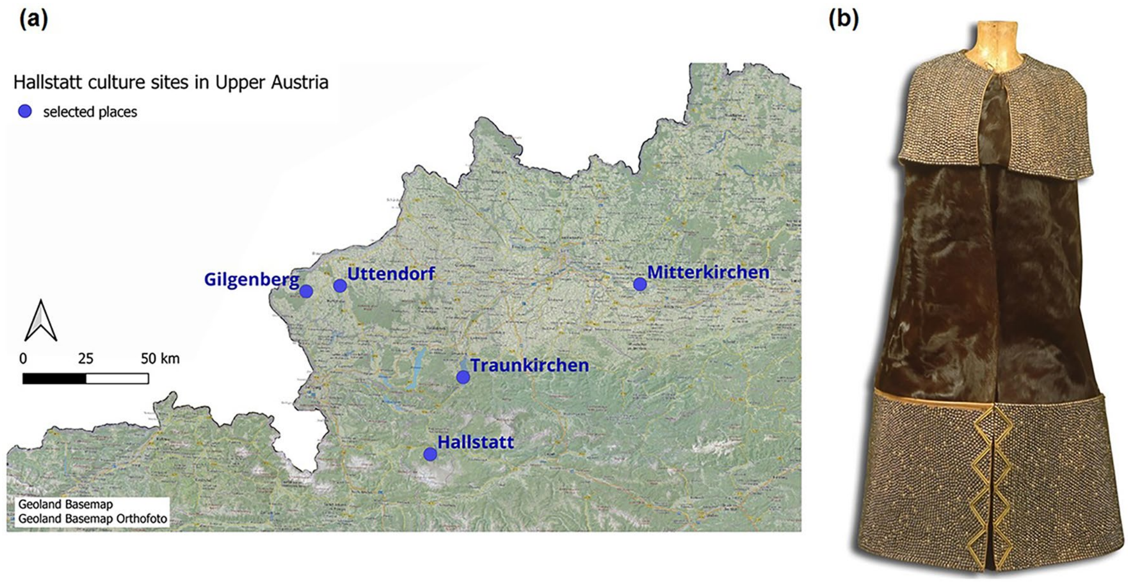

Fig. 1 (**a**) Map showing Mitterkirchen in relation to selected Hallstatt culture sites, (**b**) reconstructed coat (© „OÖ Landesmuseum/OÖLKG“). Reprinted with permission conveyed by author Jutta Leskovar on behalf of OÖ Landesmuseum/OÖLKG.

mound in Schandorf have been examined by material investigations [17].

Experimental Procedures

The five provided buttons were first examined by nondestructive methods using micro-computed tomography (micro-CT) (VISCOM X8060) and 3D digital microscopy (3D-DM) (KEYENCEVHX-5000). Two of the buttons were selected for metallographic studies.

Since conventional metallography with cutting and metallographic preparation was not possible for such small objects, they were cold mounted twice in epoxy resin. Before the second embedding was performed, a cut was made as parallel as possible to the eyelet of the button. The metallographic preparation and documentation took place in several stages. After the desired coarse removal of material, polishing was carried out with 9, 3 and 1 µm diamond suspension. Klemm 2 or $(NH_4)_2CuCl_4$ solutions were used to develop the microstructure [18]. Light optical microscope (LOM) (Olympus GX51with an associated CCD camera) and scanning electron microscope (SEM) (company FEI) with backscattered electron mode (BSE) and energy-dispersive X-ray analysis (EDX) (company EDAX) were used for the investigations. The SEM worked in low vacuum mode to avoid charging. 20 or25 kV were selected as the acceleration voltage for the electrons. Additionally, X-ray fluorescence examination (XRF) for an average analysis was applied. (Panalytical Axios Advanced machine, Rh tube, excitation voltage of 50 kV, tube current 50 mA, < 10 Pa vacuum. The PanalyticalOmnian standards and Panalytical Omnian software were used.)

Results and Discussion

Nondestructive Investigation Methods

The front and back sides of the buttons were documented using 3D-DM. The buttons have an average diameter of 7 mm (Fig. 2). The smallest diameter was 6.2 mm and the largest was 8 mm. Due to a certain eccentricity of the buttons, fluctuations in diameter are observed.

The eyelets are located centrally at the inside of the buttons which was shown in the SEM images in (Fig. 2) and additionally different amounts of corrosion products are visible, which is probably due to different cleaning and restoration.

From a lot of micro-CT images, different sections were selected for each button (Fig. 3). The positions of the eyelets can be clearly seen in the cross sections. The longitudinal cuts show no irregularities in the material, at the transition from the eyelet to the button cap. This is an obvious indication that the buttons were produced by casting.

For metallographic examinations, the buttons M643-A and M643-E were selected.

Metallographic Investigations of Two Buttons

To determine the chemical composition of the buttons, XRF analyses were carried out at the metallographically prepared cross sections. The results are summarized in Table 1.

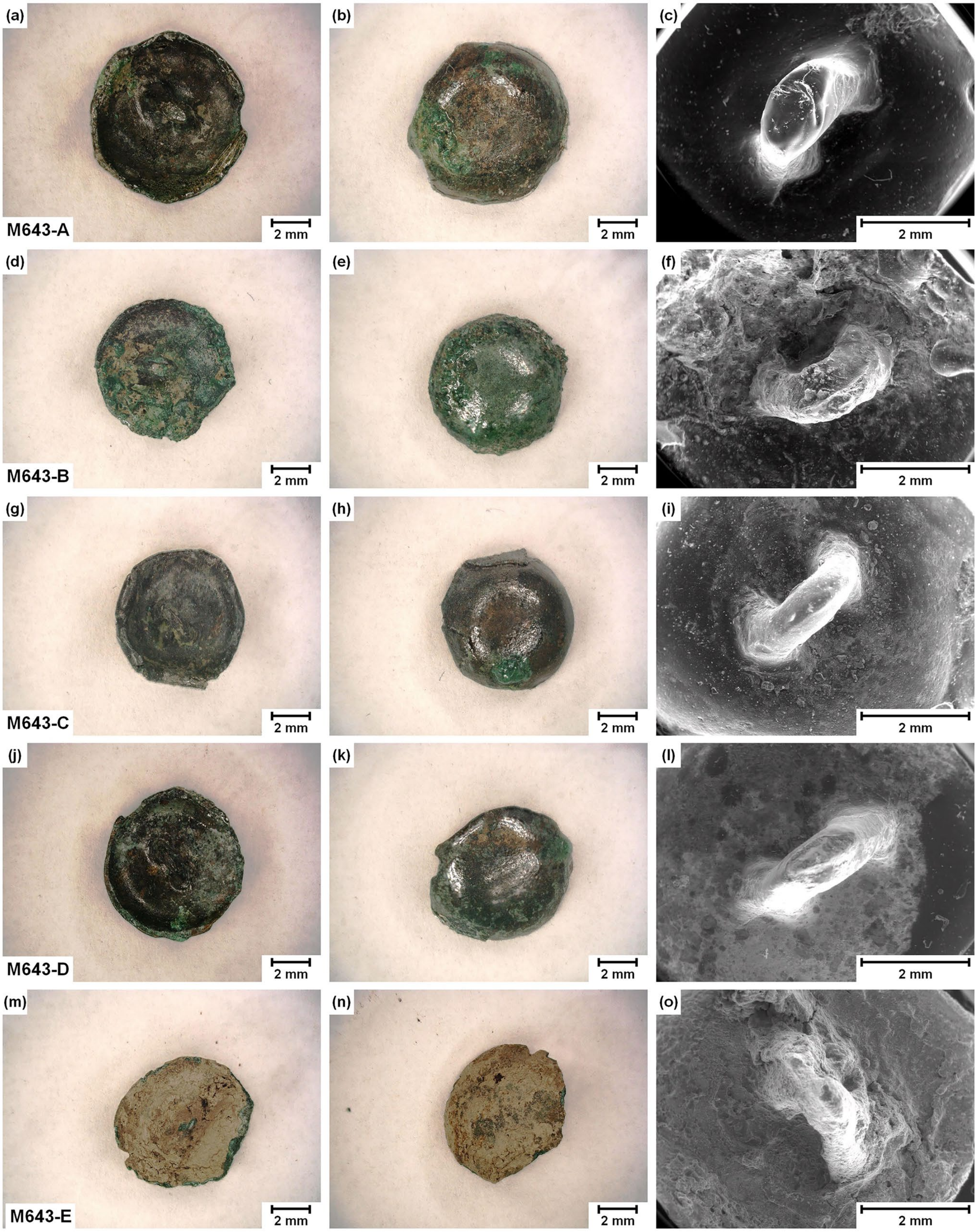

Fig. 2 Photographs from the investigated buttons. (**a–c**) M643-A, (**d – f**) M643-B, (**g–i**) M643-C, (**j–l**) M643-D, (**m–o**) M643-E. (**a** , **b**, **d**, **e**, **g**, **h**, **j, k**, **m**, **n**) 3D-DM, (**c**, **f**, **i**, **l**, **o**) SEM.

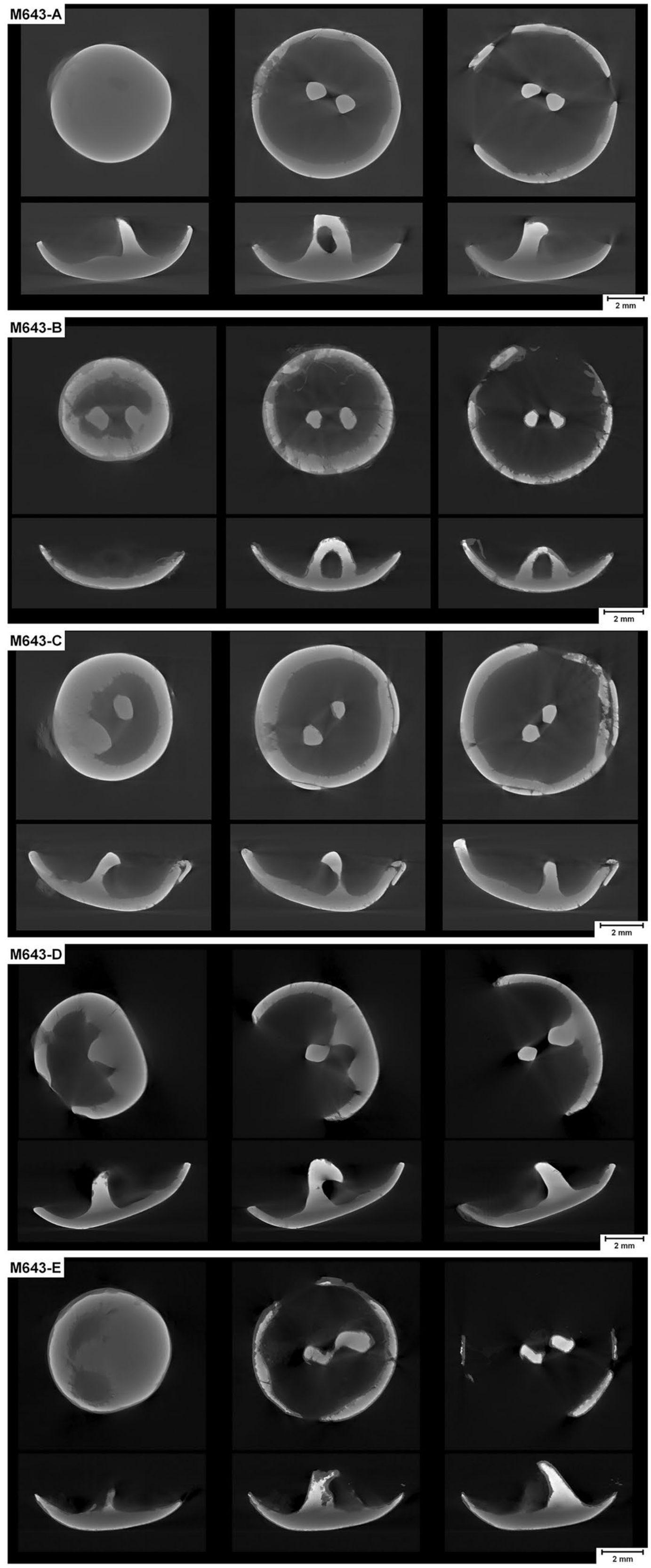

Fig. 3 CT slices at different orientations and high.

Surprisingly, Pb contents of 1.5 up to 18.8 % by weight were detected in the samples. Such high Pb contents and the large fluctuations of concentration suggest that the bronze was not obtained from fresh raw but from recycled material. Studies on hoards have shown that high concentration fluctuations are possible by using recycled material [12]. Low concentrations of As and Sb may come from the various Cu and Sn ores, but it is also suspected that other ores such as PbS or Sb_2S_3, were intentionally added to the copper [19, 20].

The measured Sn contents of 15.1 and 12.7% by weight cannot be viewed as composition of the bronze alloy, since corrosion products were also present and has to be taken into account. It is known that when Sn bronze corrodes, Sn accumulates as SnO_2 in the corrosion products [21, 22]. The other measured trace impurities are present in concentrations of less than 0.6% by weight.

At first, a plane in the cap area of the button M643-A was examined and different corroded areas are visible (Fig. 4). According to the SEM-EDX analyses, the metallic bulk of the bronze contains about 10 wt.% Sn and 2 wt.% S.

The α-phase of the bronze has a grain size between 50 and 150 µm (Fig. 4b, c).

Other components of the microstructure are Cu_2S, Pb and occasionally $Cu_{41}Sn_{11}$ (Fig. 4c, d).

One of the corroded locations is an approximately 500 µm void with corresponding corrosion products, which consist of Cu_2O (in polarized light red) and malachite ($Cu_2(CO_3)(OH)_2$) (in polarized light green) (Fig. 4e–g). The Sn content in the corrosion products was enriched up to 50 wt.%.

Grain boundary corrosion was found as well as cracks with a depth up to 500 µm (Fig. 4h–j). The crack does not run vertically into the metal but at an angle of about 45°. This form of corrosion usually follows mechanical stresses in the metal, which is caused by manufacturing or use.

A section through the eyelet of the button is shown in Fig. 5.

Table 1 XRF measurements on the metallographically prepared surfaces, of the buttons M643-A and M643-E (wt.%).

Element	M643-A	M643-E
Cu	83,01	66,80
Sn	15,06	12,68
Pb	1,50	18,80
S	0,18	0,09
Ni	0,08	0,11
Fe	n.n.	0,23
As	n.n.	0,06
Si	0,18	0,60
P	n.n.	0,07
Ca	n.n.	0,30
K	n.n.	0,09
Al	n.n.	0,17

After polishing the cross section is quite homogeneous (Fig. 5a). Larger areas of corrosion can be seen in- and outside of the cap (Fig. 5b). It seems that corrosion started along the grain boundaries and then the corrosion zone expanded further (Fig. 5c). An element distribution of this area was also made using SEM-EDX (Fig. 6). It can be clearly seen that mainly Sn and O are present in the corroded areas and Cu is not present as an oxide. Sulfur in the bronze is probably present as Cu_2S and is evenly distributed in small precipitates.

Furthermore, cracks with corrosion products were found inside the eyelet (Fig. 5d). The image of the etched sample (Fig. 5e) shows that the grain size in the cap area is smaller than in the eyelet (Fig. 5f –i) and many twins are visible (Fig. 5i). Isolated $Cu_{41}Sn_{11}$ accumulations, with a size of 40 up to 60 µm, were found rarely near the surface (Fig. 5j, k).

In the same way, two planes of the M643-E button were documented. The first cut was in the area of the cap (Fig. 7). After polishing, a striking thick corrosion layer can be seen on this button, especially at the outside (Fig. 7a, b). Many dark gray inclusions are observable in the polished metallic area (Fig. 7c). The etched sample shows a uniform α-phase microstructure with grain sizes between 50 and 100 µm and some twin grain boundaries (Fig. 7d).

Using SEM-EDX, it was possible to prove that the inclusions are Pb (light spots in SEM-BSE) (Fig. 7e, f).

In the SEM-BSE image the corroded areas appear in two layers (Fig. 7e, f). The outer layer is brighter due to a higher Sn content (25 wt.%) compared with the darker layer (17 wt.%). This two-layered structure cannot be detected in the LOM and with polarized light only malachite (green) but no Cu_2O was observed (Fig. 7g, h).

A second plane was prepared in the area of the eyelet (Fig. 8a).

In addition to Pb and $Cu_{41}Sn_{11}$ precipitates, the structure in this area shows some voids with sizes of up to 20 µm (Fig. 8b). The voids can be interpreted as shrink holes that were formed during bronze solidification. After etching, a uniform structure of α-phase with grain sizes of up to 150 µm can be seen (Fig. 8c). In the edge zones of the cap, the structure is finer-grained than in the center (approx. 20 µm) and no voids are detected (Fig. 8d, e). This could indicate post-processing of the edge.

The eyelet area is heavily corroded (Fig. 8f, g, h). The metallic area correlates with the alloy of the button. As can be seen from the polarized light image, the corrosion layer is malachite (green) and again, no Cu_2O is detected (red). Since metallic bronze is still present within the corrosion products, it can be concluded that preferential corrosion occurs along the grain boundaries. In the SEM image, clear differences in brightness can be seen in the corrosion layer with higher Sn concentrations at the rim (Fig. 8h). To illustrate the previous description, an EDX element distribution

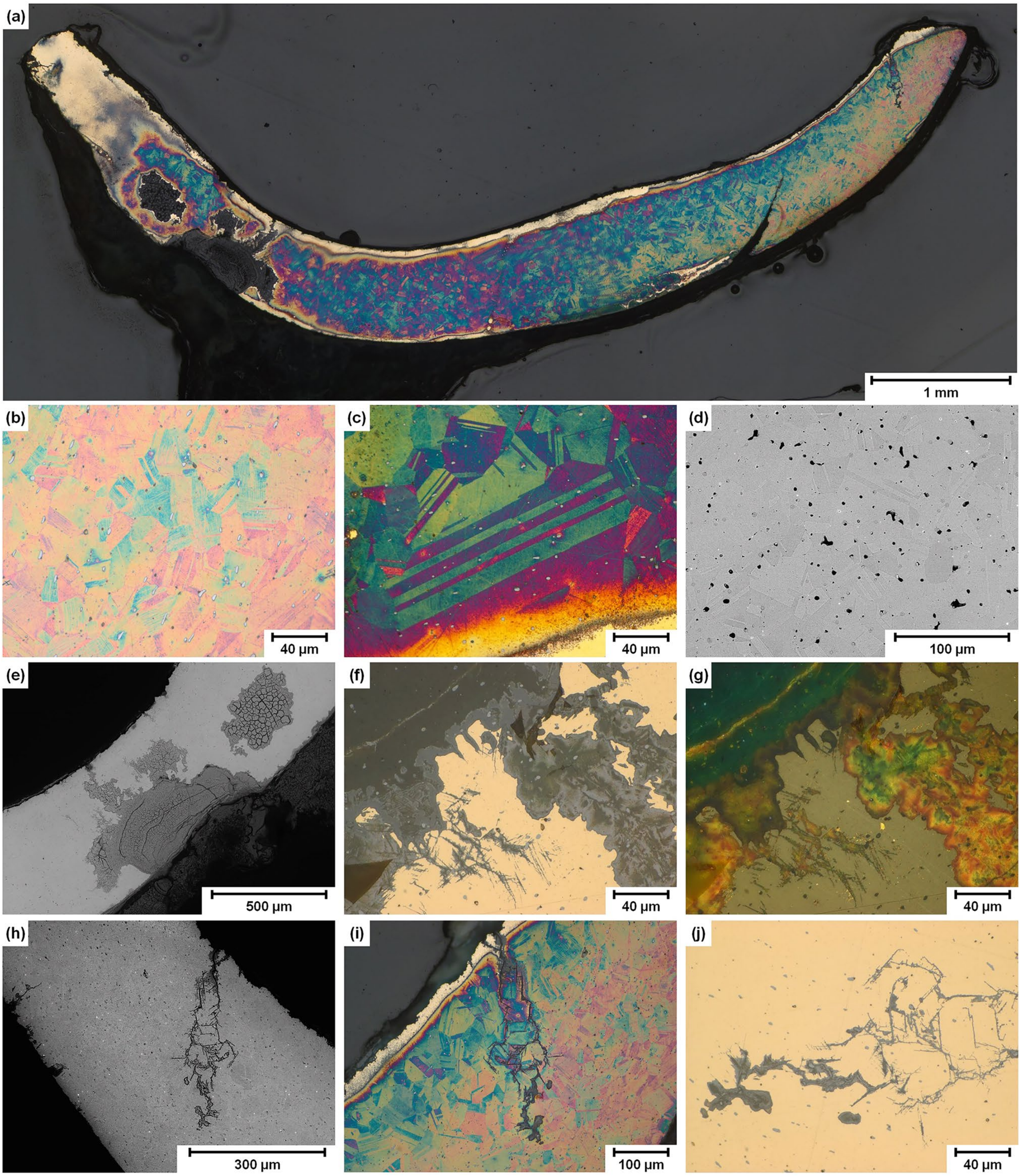

Fig. 4 Button M643-A. Plane at the cap. (**a**) overview, Klemm2 etched (**b**–**j**) various microstructures, (**b**, **c**, **i**) Klemm2 etched, LOM, (**f**, **g**, **j**) polished, LOM, (**g**) polarized light, LOM, (**d**, **e**, **h**) SEM.

was recorded from a region of the corrosion layer (Fig. 9). Clearly visible is Sn enrichment at the rim of the corroded layer. Sulfur and lead impurities of the bronze were additionally shown in the mapping. However, it must be noted that the X-ray peaks of Pb and S are very close to each other, and therefore, confusion between Pb and S is possible. Phosphorus was also measured, maybe originated from the leather coat.

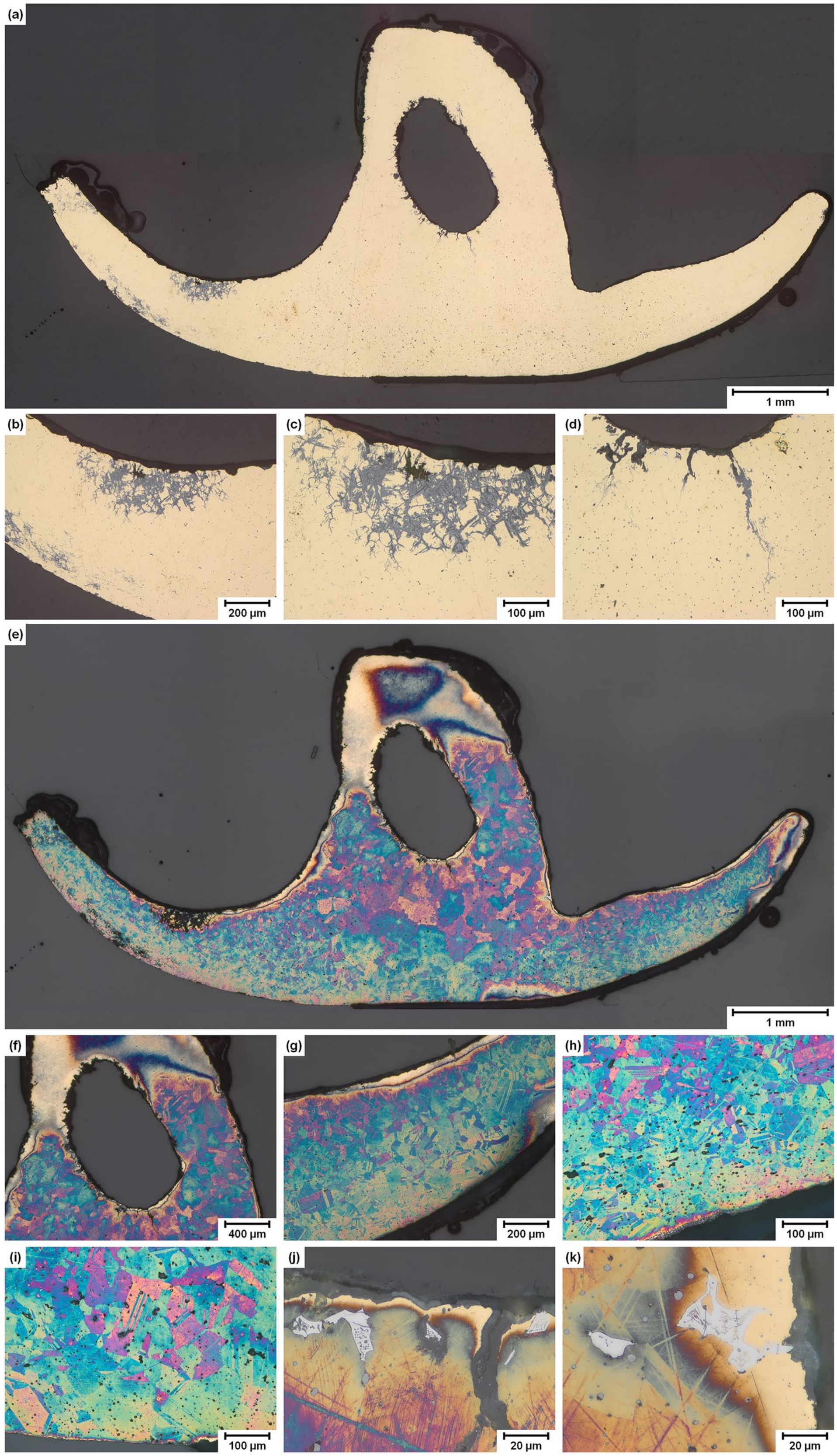

Fig. 5 Button M643-A. Plane at the eyelet. (**a**-**d**) polished sample, LOM, (**e**-**k**) Klemm2 etched, LOM.

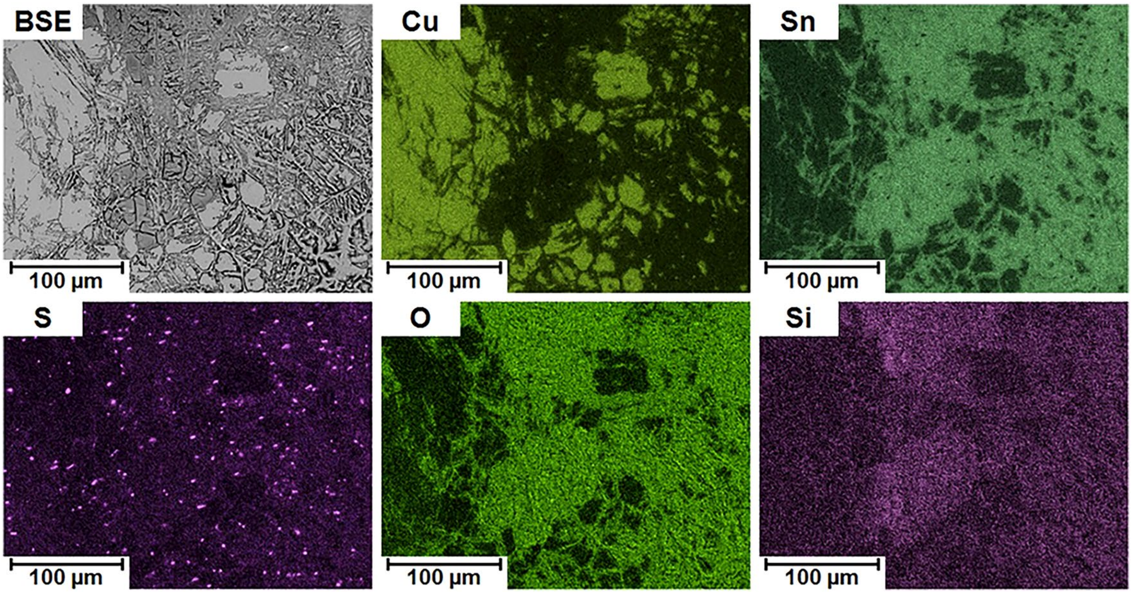

Fig. 6 Button M643-A. SEM-EDX element distribution of a corroded spot.

The buttons were probably manufactured by casting and some mechanical post-processing. There was no evidence of soldering or riveting in either the CT or the metallographic examinations. The structure of the bronze appears to be evenly recrystallized α–phase grains and there is no noticeable dendritic solidification structure as in case of the Schandorf buttons [17].

This could be explained by the fact that the burial in Schandorf was a cremation and that in Mitterkirchen was an inhumation. Experimental archeology studies have shown that during a cremation temperatures can exceed the melting point of bronze [23]. Therefore, it is impossible to determine whether a solidification structure was formed during the production of the buttons or during cremation.

Conclusions

Five buttons of a magnificent coat from the Hallstatt culture were investigated.

In addition to characterize the metal alloy, an attempt was made to find out how the buttons were manufactured. Not only a casting process but also soldering or riveting would be possible.

After examination of all buttons using computed tomography and 3D-DM or SEM, two buttons were selected for metallographic investigations. For both the microstructures were documented on two planes.

XRF analyzes on the metallographic sections show very different alloy compositions in terms of Sn and Pb additions. Thus, it can be concluded that the buttons were, at least partially, made from recycled material and not at the same time. This seems logical for the production of approximately 3000 coat buttons. The microstructure of the bronze alloys is a duplex grain-sized α-phase with twins and mainly Pb as well as $Cu_{41}Sn_{11}$ precipitates.

The most likely manufacturing method is casting and finishing. It is noticeable that only malachite and no Cu_2O were found in the patina layer. The corrosion product Cu_2O was only found in cracks. The phenomenon that Sn becomes enriched in the corrosion layer was also observed in these samples, with an outer corrosion layer containing significantly more Sn than the inner one. Other observed corrosion types are grain boundary corrosion and stress-induced corrosion.

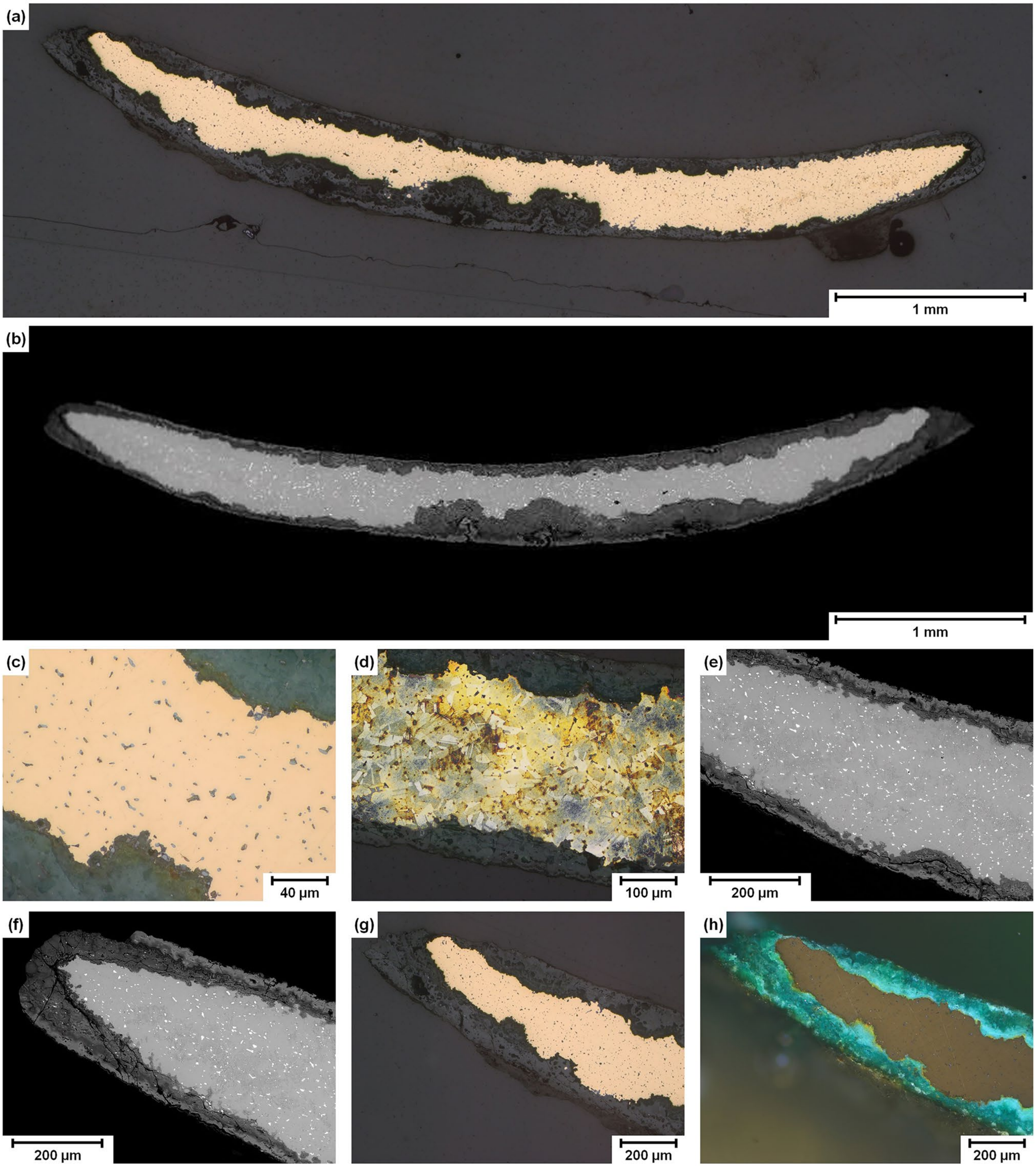

Fig. 7 Button M643-E. Plane at the cap. (**a**, **b**) overviews,. (**a**) polished, LOM, (**b**) SEM, (**c**, **d**, **e**) bronze microstructure, (**c**) polished, (**d**) $(NH_4)_2CuCl_4$, (**e**) SEM, (**f**, **g**, **h**) corrosion layer, (**f**) SEM, (**g**) polished, LOM, (**h**) polarized light, LOM.

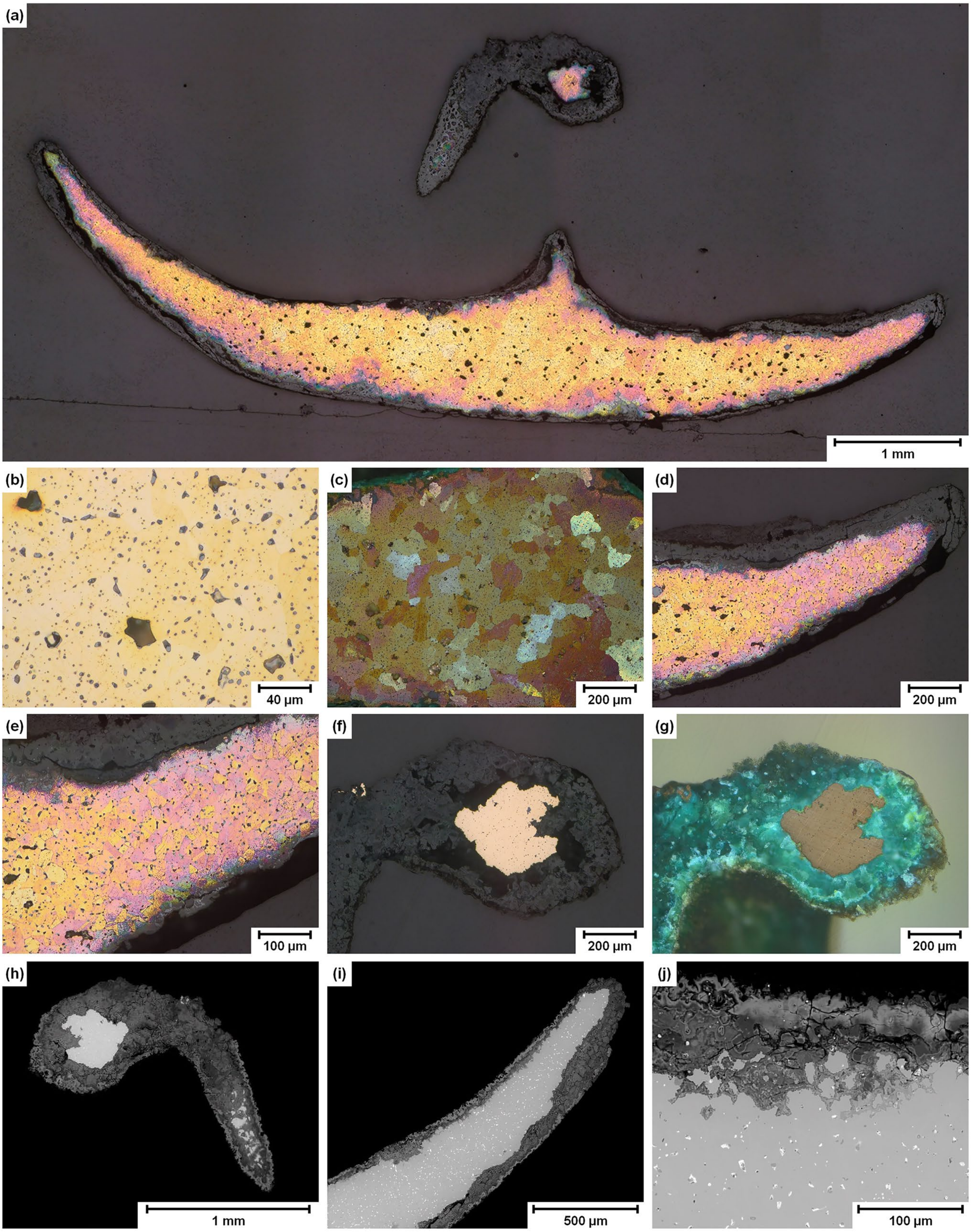

Fig. 8 Button M643-E. Plane at the eyelet. (**a**) overview, LOM, (**b**–**g**) microstructures, LOM, (**a**, **c**, **d**, **e**) $(NH_4)_2CuCl_4$ etched, (**b**, **f**, **g**) polished, (**c**, **g**) polarized light, (**h**–**j**) SEM.

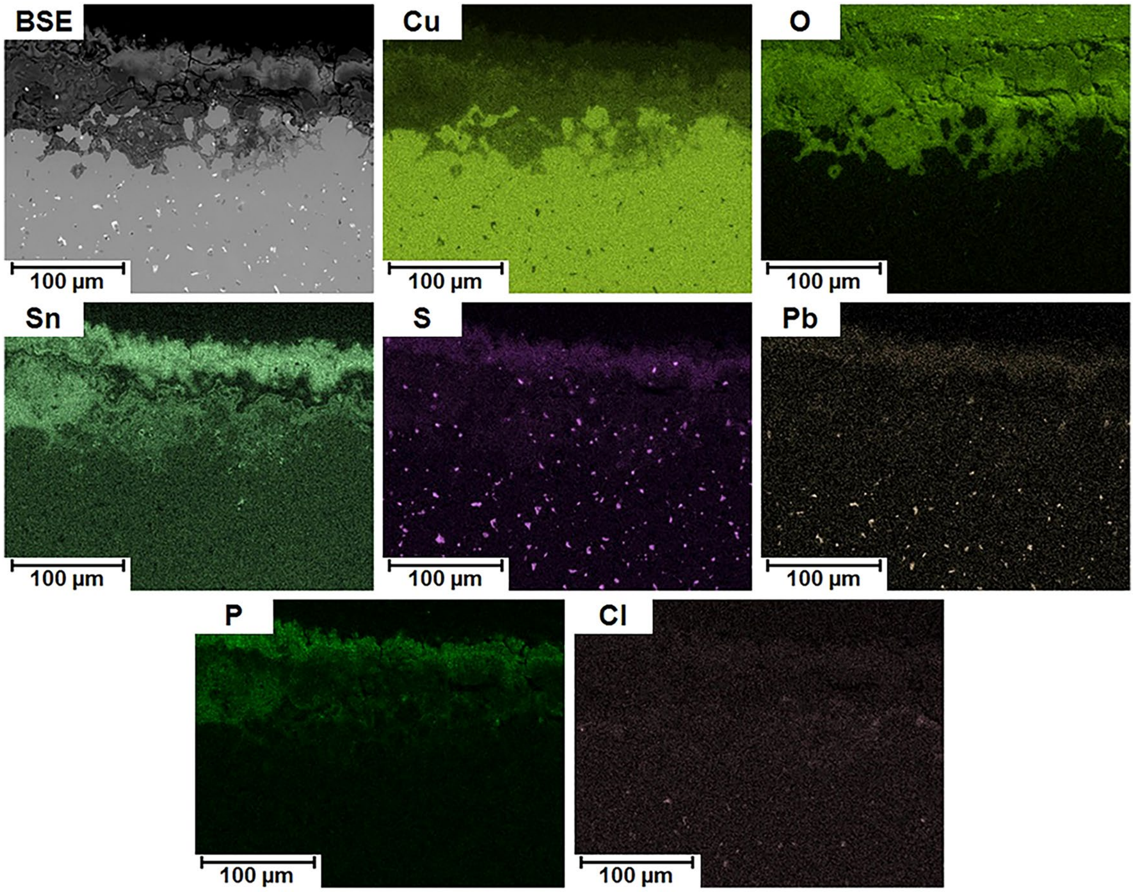

Fig. 9 Button M643-E. SEM-EDX element distribution of the corrosion layer.

Acknowledgments We would like to thank Mr. Adrian Wengler, who helped with the sample preparation for his bachelor thesis. We also thank Dr. Johannes Zbiral for the XRF measurements.

Funding Open access funding provided by TU Wien (TUW). The authors acknowledge TU Wien Bibliothek for financial support through its Open Access Funding Program.

References

1. H. Reschreiter, K. Kowarik, Bronze age mining in hallstatt a new picture of everyday life in the salt mines and Beyond. Archaeologia Austriaca. **103**, 99–136 (2019)
2. M. Egg, Die hallstattzeitlichen Hügelgräber bei Helpfau- Uttendorf in Oberösterreich. Jahrbuch RGZM. **32**, 323–393 (1985)
3. R. Schumann, *Die Siedlungsarchäologie der Bronze- und Urnenfelderzeit in Oberösterreich und die Ausgrabungen von Gilgenberg-Bierberg*, Fundberichte aus Österreich, Materialheft Reihe A, **23**, (2016)
4. J. Leskovar, R. Schumann, *Das älterhallstattzeitliche Gräberfeld von Mitterkirchen. Ein Beitrag zur frühen Eisenzeit (Ha C) im oberösterreichischen Donauraum.* Studien zur Kulturgeschichte von Oberösterreich **53**, 2023
5. R. Schumann, J. Leskovar, M. Marschler *Neue Forschungen zum hallstattzeitlichen Grabhügelfeld von Mitterkirchen (Oberösterreich)*, in: F: Nikulka/D. Hofmann/R. Schumann (eds), Menschen – Dinge – Orte. Aktuelle Forschungen des Instituts für Vor- und Frühgeschichtliche Archäologie der Universität Hamburg, p. 133-140 (2018)
6. J.-W. Neugebauer, *Bronzezeit in Ostösterreich* (Verlag Österreichisches Pressehaus, Wissenschaftliche Schriftenreihe Niederösterreich, 1994)

7. M.L.S. Sørensen, K. Rebay-Salisbury, *Death and the body in Bronze Age Europe From inhumation to cremation* (New York, Port Melbourne, New Delhi, Singapore Cambridge University Press, Cambridge, 2023)
8. M. Pertlwieser, Frühhallstattzeitliche Herrschaftsgräber bei Mitterkirchen (Oberösterreich). Antike Welt. **18**, 48–56 (1987)
9. M. Pertlwieser *Frühhallstattzeitliche Wagenbestattungen in Mitterkirchen*, in: Prunkwagen und Hügelgrab, Kultur der frühen Eisenzeit von Hallstatt bis Mitterkirchen, Katalog des OÖ Landesmuseums, Linz, p. 55-70 (1987)
10. R.F. Tylecote, *The early history of metallurgy*, London–New York, (1987)
11. R. Haubner, Die prähistorische Kupfermetallurgie – allgemeine Betrachtungen. BHM Berg- Huettenmaenn. Monatsh. **166**, 343–351 (2021)
12. R. Haubner, S. Strobl, Investigations on copper cast cakes, sickle fragments and a spout axe of the hoard find from Drassburg/Burgenland. Metallogr. Microstruct. Anal. **12**, 187–201 (2023)
13. M. Radivojević, B.W. Roberts, E. Pernicka et al., The provenance, use, and circulation of metals in the european bronze age: the state of debate. J. Arch. Res. **27**, 131–185 (2019)
14. R. Haubner, For THEY do not know what THEY are doing. Pract. Metallogr. **60**, 331–342 (2023)
15. F.R. Herrmann, Fürstengrabhügel 2 am Glauberg in seinem Umfeld In: Der Glauberg in Keltischer Zeit Zum neuesten Stand der Forschung Fundberichte Hessen. Beiheft. **6**, 89–138 (2008)
16. M. Fritzl, *Die mehrfach belegten Gräber des urnenfelderzeitlichen Gräberfeldes von Inzersdorf ob der Traisen, Niederösterreich*. Master Thesis, University of Vienna (2017)
17. R. Haubner, Garment buttons from a Hallstatt period tumulus. Pract. Metallogr. **60**, 276–288 (2023). https://doi.org/10.1515/pm-2022-1021
18. G.F. Vander Voort, *Metallography – Principles and Practice*, ASM International, 3rd printing, (2004) https://doi.org/10.31399/asm.hb.v09.a0003752
19. R. Haubner, F. Ertl, S. Strobl, Examinations of a Bronze Ingot Made of Fahlore. Pract. Metallogr. **54**, 107–117 (2017)
20. R. Haubner, S. Strobl, M. Thurner, H. Herdits, Ein Kupfergusskuchen mit hohem Antimongehalt aus Velem/Westungarn. BHM Berg Huettenmaenn. Monatsh. **165**, 453–460 (2020)
21. R. Haubner, S. Strobl, P. Trebsche, *Metallographic analyses from the late Urnfield period copper mining settlement at Prigglitz-Gasteil in Lower Austria*, in: R. Turck, T. Stöllner and G. Goldenberg (Eds), Alpine Copper II – Alpenkupfer II – Rame delle Alpi II – Cuivre des Alpes II. New Results and Perspectives on Prehistoric Copper Production, Der Anschnitt, Beiheft 42, (2019), Verlag Marie Leidorf, Bochum. p. 323-332
22. R. Haubner, S. Strobl, P. Trebsche, Analysis of Urnfield period bronze droplets formed during casting. Mater. Sci. Forum. **891**, 41–48 (2017)
23. R. Haubner, S. Strobl, M. Fritzl, M. Konrad, Changes in the microstructure of bronze parts during experimental archaeological cremations. BHM Berg Huettenmaenn. Monatsh. **169**, 104–110 (2024). https://doi.org/10.1007/s00501-024-01427-x